Z. Physik 263, 251–266 (1973)

States of ^{5}He and ^{8}Be from the Reaction ^{7}Li + d

Evaluation of α-α-Coincidence Spectra

D. Kamke

Institut für Experimentalphysik der Ruhr-Universität Bochum, Bochum

Received June 6, 1973

Nuclear reactions of deuterons with ^{7}Li have been used in order to determine properties of the intermediate nuclei ^{8}Be and ^{5}He. Of particular interest are locations and widths of the ground state and first excited state of ^{5}He, and of the second excited state of ^{8}Be. In a complete α-α-coincidence spectrum, however, overlapping of the coincident rates restricts very much the evaluation of such spectra. Particularly important is the velocity of the over-all center of mass which may cause unfavourable conditions for reliable determinations of the wanted data.

1. Introduction

The nuclear reactions ^{7}Li$(d, n)^8$Be(2α) and ^{7}Li$(d, \alpha)^5$He$(n\alpha)$ are easily accessible because of the high Q-value of 15.122 MeV [1]. They are capable of giving results for states of the ^{5}He-nucleus as well as of the ^{8}Be-nucleus, if a complete experiment is performed. This means that two particles of the exit channel must be recorded (either two α-particles or one α-particle and the neutron), and the coincidence rate must be analyzed with respect to the intermediate states. The main interest is with the first excited state of ^{5}He$(1/2, -)$ and with the second excited state of ^{8}Be$(4, +)$, the locations and widths of which have not yet been determined uncontestedly. The main reason is that even in a two-parameter experiment the proper isolation of the corresponding lines suffers from superpositions of the α-particles from both exit channels.

States of ^{5}He. The most recent paper by Gil, Marquez, Québert and Sztark [2] ascribes to the *first excited state* of ^{5}He the excitation energy $E^* = 2.6$ MeV and the width $\Gamma = 7$ MeV. The underlying experiment is complete in that an α-α-coincidence spectrum is recorded. Strauss and Friedland [3] also measured α-α-coincidences and reported an excited state at $E^* = 2.9$ MeV and another one at 4.8 MeV. Fessenden and Maxson [4] evaluated such spectra as well and found $E^* = 2.6$ MeV, $\Gamma = 4.0$ MeV. Assimakopoulos, Gangas, Kossionides and Democritus [5] located the first excited state in ^{5}He at 5.2 MeV with $\Gamma = 5.6$ MeV, again from α-α-coincidence work.

State of ^{8}Be. Hofmann and Kamke [6] evaluated their α-α-coincidence spectra with respect to the second excited state in ^{8}Be and found $E^* = 11.4$ MeV, $\Gamma = 2.8$ MeV for this 4,+state. Strauss and Friedland [3] reproduced the experimental conditions of this experiment and remarked that probably the spectra should rather have been evaluated with respect to ^{5}He, and then gave the data reported on above.

There has been done quite some more experimental work on both reactions. Various angular correlations of the α-α- and n-α-radiations were measured [7]. Valković, Jackson, Chen, Emmerson and Phillips [8] took many coincidence spectra at bombarding energies up to 4 MeV and found even the 16.63, 16.93 and 20 MeV states of ^{8}Be, whereas the 11.4 MeV state and states of ^{5}He could not be located precisely enough. The authors say that ambiguities will remain due to multiple appearance of the states. In the literature it seems to be the only remark on difficulties that are inherent to this kind of experimental technique, and which are sometimes impossible to avoid or to circumvent (see also Ref. [11]). Since in our laboratory many coincidence spectra for various purposes have been taken and evaluated it was felt worthwhile to report on some basic ideas on the problems one encounters. It should be remarked that the following considerations are of purely kinematical nature.

2. Appearance of Levels in the Center of Mass System

It is well known that in the center of mass system of a three particle nuclear reaction

$$a + A \rightarrow b_3 + B_{12} \rightarrow b_3 + b_1 + b_2$$

an intermediate state B_{12} leads to a sharp energy of b_3. If the energies of b_1, b_2 and b_3 are plotted in a triangular diagram, the shape of which only depends on the masses m_1, m_2 and m_3 [9], and if reduced energies ε_1, ε_2, ε_3 are used, all possible configurations lie within the inscribed circle of that triangle (Fig. 1). A sharp state of B_{12} gives rise to coincidence

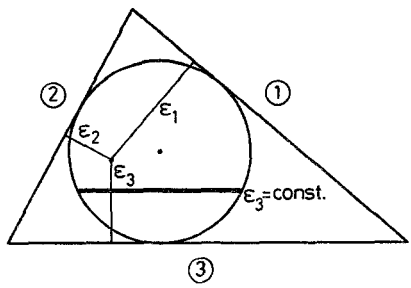

Fig. 1. Triangular energy diagram with reduced energies

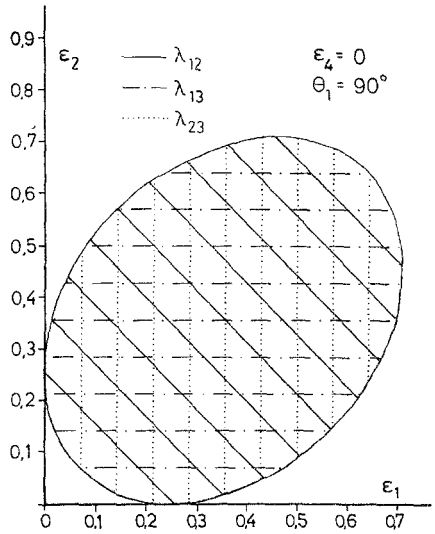

Fig. 2. A subsystem in the exit channel of the reaction ^{7}Li+d leads to coincident events along the straight lines for constant λ_{12}(^{8}Be) and λ_{13}, resp. λ_{23}(^{5}He) if the velocity of the c.m. is zero

rates, which, when plotted as heights give the impression of a sharp ridge along the line $\varepsilon_3 = \text{const}$. The same is true, if instead of b_1 and b_2 another group of particles, (23) or (31), is generated from the decay of another intermediate nucleus B_{23} or B_{31}. The population of the energy diagram (Dalitz-plot) is measured by using two detectors at certain directions with respect to an incoming beam. The *kinematical curve*, determined by constant angle ϑ_{12} between the detectors, gives the kinematically possible location of coincidences. Where this curve intersects a straight line belonging to an intermediate state, one finds coincident events. The total population of the diagram is therefore measured by changing the angle ϑ_{12} between the detectors.

The energy diagram is degenerate to a certain extent. Firstly it depends only on the angle ϑ_{12} between two detectors. Secondly the straight lines belonging to an intermediate state are covered twice. Both degeneracies disappear when the velocity of the c.m. is different from zero.

The simple picture with straight lines traversing the energy triangle (Fig. 2) facilitates the evaluation. It is true only in the center of mass system, within which measurements are never done. It may be approximated, however, by using very low energies of the incoming particle

beam. Sometimes this is possible, if the reaction has a relatively high Q-value. For instance the reaction $^{11}B(p, \alpha)2\alpha$ has been measured with as low a proton energy as 100 keV.

3. Appearance of Levels in the Laboratory System

The transformation from the c.m. system into the laboratory system seems to be simple. One has to add the velocity of the c.m. to all particle velocities. Difficulties, that influence the chance for unique evaluations of the spectra, are due to the fact that one has a two step process. At any stage particles may be emitted in any direction. The final result now depends on some more parameters that may be chosen by the experimentalist. These are for instance the directions where detectors are set up in the laboratory system, for the kinematical curve now not only depends on the angle between the detectors but also on the direction itself. Furthermore, one wants to discuss the influence of the velocity of the c.m. in order to be able to choose one that optimizes the evaluation of the data. Finally one wants to discuss the influence of the amount of energy contained in a subsystem. Since the task is to determine this energy experimentally one needs a complete survey of the kinematics in the laboratory system as a function of the parameters just mentioned.

(a) The following calculations are aimed at receiving the relation between the energies of two particles (number 1 and 2) in the *laboratory system* if an arbitrary, yet fixed amount of energy is contained in the (12) system. This arbitrary amount will be described by a suitably chosen parameter λ ($0 \leqq \lambda \leqq 1$). A second parameter, called ε_4 later on, is of equal importance. It measures the amount of energy of the c.m., resp. the velocity of the c.m. The value $\varepsilon_4 = 0$ automatically gives the center of mass description.

It has proven advantageous to introduce so-called reduced energies. They will allow to give concise pictures of energy relations even in the case when the energy of the c.m. is large, though we do not discuss relativistically high velocities. We use relations that have been described in preceding papers [10]. They will be repeated only as far as is necessary. In the laboratory system (l.s.) the momenta of the particles 1, 2 and 3 are $\boldsymbol{P}_1$, $\boldsymbol{P}_2$, $\boldsymbol{P}_3$. The momentum of the c.m. is $\boldsymbol{P}_s$, where

$$\boldsymbol{P}_1 + \boldsymbol{P}_2 + \boldsymbol{P}_3 - \boldsymbol{P}_s = 0, \tag{1}$$

and $m_s = m_1 + m_2 + m_3$ is the mass of the c.m. The sum of the kinetic energies is $E_1 + E_2 + E_3$. We add the energy of the c.m. and define

$$T_4 = E_1 + E_2 + E_3 + E_s = Q_3 + E_a + \frac{m_a}{m_a + m_A} E_a, \tag{2}$$

where it has been assumed, that the Q-value of the reaction is Q_3. The energy of the incoming particle a in the l.s. is E_a, and the target nucleus has mass m_A.

Eqs. (1) and (2) would be exactly the same if we had to deal with a system of four particles in its c.m. system, only the index s would be replaced by 4 and $\boldsymbol{P}_s$ by $-\boldsymbol{P}_4$. This viewpoint allows the definition of maximum energies,

$$E_{i,\max}=\frac{M_4-m_i}{M_4}T_4=\frac{T_4}{h_i},\qquad i=1,2,3,4, \tag{3}$$

with $M_4=m_1+m_2+m_3+m_4$ (in our case $m_4=m_1+m_2+m_3=m_s$). A particle attains its maximum energy if the remaining system of three particles in the c.m. system moves opposite to the one selected, *and* has internal energy zero. It is only natural to then define the reduced energies by

$$\varepsilon_i=E_i/E_{i,\max}. \tag{4}$$

The energy Eq. (2) receives the form

$$\frac{\varepsilon_1}{h_1}+\frac{\varepsilon_2}{h_2}+\frac{\varepsilon_3}{h_3}+\frac{\varepsilon_4}{h_4}=1. \tag{5}$$

The basis for the above mentioned conciseness is Eq. (5). It shows that the ε_i are confined to the inner part of a tetrahedron of energies [10].

Corresponding to our program we take ε_4 as the parameter that gives the velocity of the c.m., and we only have to define yet the inner parameters that describe the energy contents of an enclosed system of two particles.

(b) The *inner parameter* λ_{12} is defined in connection with the particle group (12) by writing a certain set of equations, which define relative momenta,

$$\begin{aligned}
&\frac{1}{\sqrt{\mu_4}}\boldsymbol{\pi}_{12}=\sqrt{\mu_{12}}\left(\frac{\boldsymbol{P}_1}{m_1}-\frac{\boldsymbol{P}_2}{m_2}\right)\\
&\frac{1}{\sqrt{\mu_4}}\boldsymbol{\pi}_{12,3}=\sqrt{\mu_{12,3}}\left(\frac{\boldsymbol{P}_1+\boldsymbol{P}_2}{m_1+m_2}-\frac{\boldsymbol{P}_3}{m_3}\right)\\
&\frac{1}{\sqrt{\mu_4}}\boldsymbol{\pi}_{123,4}=\sqrt{\mu_{123,4}}\left(\frac{\boldsymbol{P}_1+\boldsymbol{P}_2+\boldsymbol{P}_3}{m_1+m_2+m_3}-\frac{\boldsymbol{P}_4}{m_4}\right)=-\frac{\boldsymbol{P}_4}{\sqrt{\mu_{123,4}}}.
\end{aligned} \tag{6}$$

The definition of the reduced masses μ_{12}, $\mu_{12,3}$, $\mu_{123,4}$ is straightforward and corresponds to the grouping of particles (12), (12, 3) and (123, 4). Furthermore we choose

$$\mu_4^3=\frac{m_1 m_2 m_3 m_4}{m_1+m_2+m_3+m_4},$$

in order to make the Jacobian of the transformation from momenta to relative momenta equal to one.

Then the parameter λ_{12} is defined by

$$\pi_{123,4}^2=\varepsilon_4 \Pi^2, \quad \pi_{12,3}^2=\lambda_{12}(1-\varepsilon_4)\Pi^2, \quad \pi_{12}^2=(1-\lambda_{12})(1-\varepsilon_4)\Pi^2 \tag{7}$$

with

$$\frac{1}{2\mu_4}(\pi_{12}^2+\pi_{12,3}^2+\pi_{123,4}^2)=\frac{\Pi^2}{2\mu_4}=T_4.$$

Indeed λ_{12} determines the energy content of the group (12),

$$e_{12}=\tfrac{1}{2}\mu_{12}v_{12}^2=(1-\lambda_{12})(1-\varepsilon_4)T_4. \tag{8}$$

Other inner parameters λ_{23} and λ_{31} are defined by permuting the particle indices (kinematical transformations).

By computing various vector products one obtains relations interconnecting reduced energies and angles. We need here only two of them:

$$\begin{aligned}\lambda_{12}(1-\varepsilon_4)=&\frac{m_1}{\mu_{12,3}}\frac{\varepsilon_1}{h_1}+2\frac{\sqrt{m_1 m_2}}{\mu_{12,3}}\sqrt{\frac{\varepsilon_1\varepsilon_2}{h_1 h_2}}\cos\theta_{12}+\frac{m_2}{\mu_{12,3}}\frac{\varepsilon_2}{h_2}\\&+\frac{m_4\mu_{12,3}}{m_3^2}\frac{\varepsilon_4}{h_4}+2\frac{\sqrt{m_1 m_4}}{m_3}\sqrt{\frac{\varepsilon_1}{h_1}\frac{\varepsilon_4}{h_4}}\cos\theta_{14}\\&+2\frac{\sqrt{m_2 m_4}}{m_3}\sqrt{\frac{\varepsilon_2}{h_2}\frac{\varepsilon_4}{h_4}}\cos\theta_{24}\end{aligned} \tag{9}$$

and

$$\begin{aligned}&(1-\lambda_{12})(1-\varepsilon_4)\\&=\frac{\mu_{12}}{m_1}\frac{\varepsilon_1}{h_1}-2\frac{\mu_{12}}{\sqrt{m_1 m_2}}\sqrt{\frac{\varepsilon_1}{h_1}\frac{\varepsilon_2}{h_2}}\cos\theta_{12}+\frac{\mu_{12}}{m_2}\frac{\varepsilon_2}{h_2}.\end{aligned} \tag{10}$$

These are two equations for ε_1 and ε_2, when λ_{12} and the angles are known. The sum of Eqs. (9) and (10) does not depend on the inner parameter λ_{12} and gives the so-called *kinematical curve in the laboratory system*. It is a relation between ε_1 and ε_2 and some angles which are experimental parameters:

$$\begin{aligned}&\left(\frac{m_2}{\mu_{12,3}}+\frac{\mu_{12}}{m_2}\right)\frac{\varepsilon_2}{h_2}+2\left[\left(\frac{\sqrt{m_1 m_2}}{\mu_{12,3}}-\frac{\mu_{12}}{\sqrt{m_1 m_2}}\right)\sqrt{\frac{\varepsilon_1}{h_1}}\cos\theta_{12}\right.\\&\left.+\frac{\sqrt{m_2 m_4}}{m_3}\sqrt{\frac{\varepsilon_4}{h_4}}\cos\theta_{24}\right]\sqrt{\frac{\varepsilon_2}{h_2}}+\left(\frac{m_1}{\mu_{12,3}}+\frac{\mu_{12}}{m_1}\right)\frac{\varepsilon_1}{h_1}\\&+2\frac{\sqrt{m_1 m_4}}{m_3}\sqrt{\frac{\varepsilon_1\varepsilon_4}{h_1 h_4}}\cos\theta_{14}-1+\varepsilon_4+\frac{m_4\mu_{12,3}}{m_3^2}\frac{\varepsilon_4}{h_4}=0.\end{aligned} \tag{11}$$

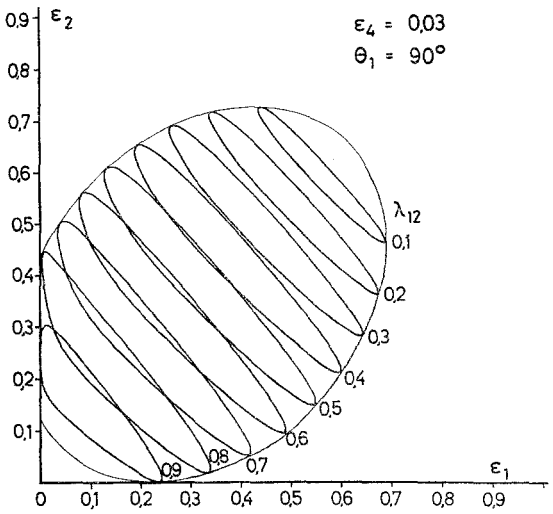

Fig. 3. The same as Fig. 2, but energy of the incoming deuteron being 1 MeV. Only lines for constant λ_{12}(^{8}Be) are drawn

This is a quadratic equation of the form

$$A\varepsilon_2+B\sqrt{\varepsilon_2}+C=0.$$

(c) The present investigation is concerned with another relation, resp. set of curves. It is received when we concentrate on such pairs of energy that result from a particular intermediate state, characterized by λ_{12}. This case cannot be dealt with in the same generality. We restrict ourselves to a kind of experiments that has been performed very often. One detector may be setup at the angle $\theta_1(=180°-\theta_{14})$. The incoming beam and the direction θ_1 define a plane in the l.s. Then detector 2 shall be located in the same plane at an angle $\theta_2(=180°-\theta_{24})$. Either we think of it as being located at fixed angle also; then we fix the kinematical curve in the ε_1, ε_2 energy diagram. Or, and this is the present case of interest, we leave it completely open where we later on will locate it. Then we are able to calculate the energy pairs that originate from the decay of an intermediate state. The assumed experimental setup is sketched in Fig. 4. We have the relation

$$2\pi=\theta_{14}+\theta_{12}+\theta_{24}, \tag{12}$$

and this is introduced in Eq. (9). Also we replace λ_{12} by the corresponding relation from Eq. (10). Further we define the parameter

$$\alpha=\frac{1}{2}\frac{\sqrt{m_1 m_2}}{\mu_{12}}(1-\lambda_{12})(1-\varepsilon_4) \tag{13}$$

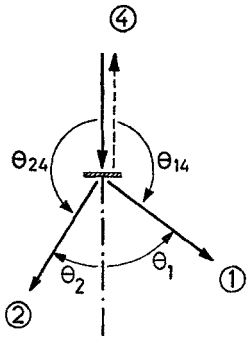

Fig. 4. Sketch of experimental situations dealt with in the text

and find

$$a+b\varepsilon_2=2\frac{\sqrt{m_2 m_4}}{m_3}\sqrt{\frac{\varepsilon_4}{h_4}}\sin\theta_{14}\sin\theta_{12}\sqrt{\frac{\varepsilon_2}{h_2}} \tag{14}$$

with

$$\begin{aligned} a=&-1+\varepsilon_4-2\alpha\left(\frac{\sqrt{m_1 m_2}}{\mu_{12,3}}-\frac{\mu_{12}}{\sqrt{m_1 m_2}}\right)\\ &+\frac{m_4\mu_{12,3}}{m_3^2}\frac{\varepsilon_4}{h_4}+\frac{m_1+m_2}{\mu_{12,3}}\frac{\varepsilon_1}{h_1}\\ &+\left(2\frac{\sqrt{m_1 m_4}}{m_3}+\frac{\sqrt{m_2 m_4}}{m_3}\sqrt{\frac{m_2}{m_1}}\right)\sqrt{\frac{\varepsilon_1\varepsilon_4}{h_1 h_4}}\cos\theta_{14}\\ &-2\frac{\sqrt{m_2 m_4}}{m_3}\alpha\cos\theta_{14}\sqrt{\frac{\varepsilon_4 h_1}{h_4\varepsilon_1}}, \end{aligned} \tag{15a}$$

$$b=\left(\frac{m_1+m_2}{\mu_{12,3}}+\frac{\sqrt{m_1 m_4}}{m_3}\sqrt{\frac{\varepsilon_4 h_1}{h_4\varepsilon_1}}\cos\theta_{14}\right)\frac{1}{h_2}. \tag{15b}$$

Taking the square of relation (14) one finds

$$(a+b\varepsilon_2)^2=c+d\varepsilon_2+e\varepsilon_2^2 \tag{16}$$

with

$$c=4\frac{m_2 m_4}{m_3^2}\frac{1}{h_4}\left(\alpha\sqrt{\frac{m_2}{m_1}}-\frac{h_1}{\varepsilon_1}\alpha^2-\frac{1}{4}\frac{m_2}{m_1}\frac{\varepsilon_1}{h_1}\right)\varepsilon_4\sin^2\theta_{14} \tag{17a}$$

$$d=4\frac{m_2 m_4}{m_3^2}\frac{1}{h_2 h_4}\left(\frac{1}{2}+\alpha\sqrt{\frac{m_1}{m_2}}\frac{h_1}{\varepsilon_1}\right)\varepsilon_4\sin^2\theta_{14} \tag{17b}$$

$$e=-\frac{m_1 m_4}{m_3^2}\frac{h_1}{h_2^2 h_4}\frac{\varepsilon_4}{\varepsilon_1}\sin^2\theta_{14}. \tag{17c}$$

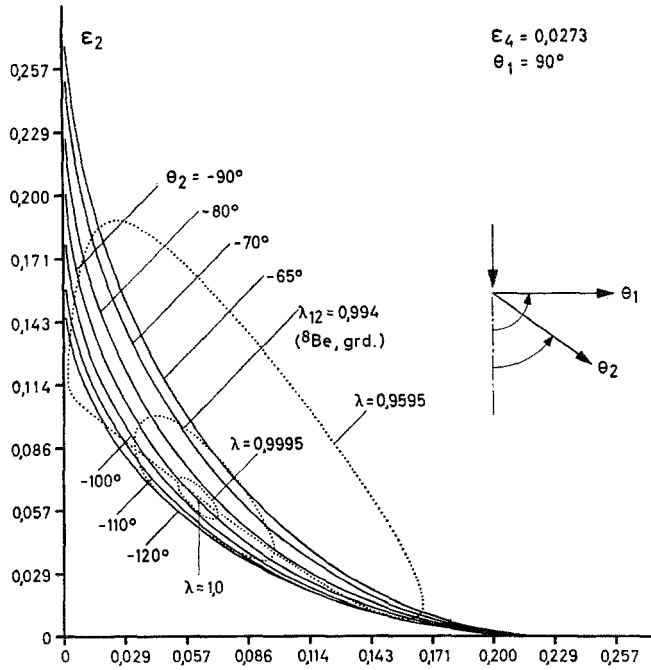

Fig. 5. Kinematical curves if one wants to measure the coincidences coming from ^{8}Be (groundstate)

So, one receives another quadratic equation, this time with λ_{12} as the parameter. It should be added, that the outcome of an experiment can only be predicted if the location of the second detector is known.

Fig. 3 contains a series of curves for constant λ_{12}, where the same masses have been used as in Fig. 2. The difference is that the energy of the incoming particle (deuteron) is assumed to be 1.0 MeV, corresponding to $\varepsilon_4 = 0.03$. Instead of straight lines we obtain a *series of closed curves.* They correspond to the straight lines that are covered twice when $\varepsilon_4 = 0$. The result therefore is the following: when the velocity of the c.m. is different from zero, coincident counts are received where the kinematical curves of the laboratory system intersect the curves that correspond to constant energy contents of the subsystem under investigation.

In order to clarify the situation further it seems worthwhile to discuss a special case in more detail. Consider the nuclear reaction

$$^7\text{Li}+d \rightarrow n+{}^8\text{Be}(\text{grd. st.}) \rightarrow n+\alpha+\alpha \qquad (18)$$

and assume that one α-detector is set up at 90° (see Fig. 5). If we want to measure the λ_{12}-curve belonging to the ground state of ^{8}Be we have to put the second detector

in the vicinity of the direction of detector no. 1, which means (with the definition of angles chosen here) that θ_2 is around $-90°$. If this angle is changed from $-65°$ to $-120°$ one obtains with each configuration coincident counts from two energy pairs, being the intersections that were mentioned above. So the total population of this particular λ_{12}-curve may be measured. The intensity distribution along that curve is the image of the angular correlation function.

From the above discussion one infers the possibility of measuring branches of the λ-curves by setting up detectors suitably. This is generally true: the clossed λ-curves separate into two nonoverlapping parts if the range of θ_1, θ_2-values is confined to certain intervals that can be found by inserting ε_1, ε_2-pairs into Eqs. (9) and (10) thereby receiving θ_{12} and θ_{24} (resp. θ_1 and θ_2).

Also another remark is in order at this place. In the quoted paper II [10] an expression for $\cos \vartheta_{3,12}$ was received. Inserting ε_1, ε_2-pairs for constant λ gives the step angle $\vartheta_{3,12}$. — Therefore the ε_1, ε_2-plane can be covered by a set of constant-λ and constant-$\vartheta_{3,12}$-curves that are bases for evaluations with respect to excited state as well as angular correlations.

(d) In the preceding section we concentrated on the subsystem (12) (later on the α-α-system) and assumed that particles 1 and 2 were recorded, whereas particle 3 escaped undetected. Nonetheless we may calculate its energy and its angle of emission by again using the set of Eqs. (6). One replaces $\boldsymbol{P}_1+\boldsymbol{P}_2$ in the second equation by $-(\boldsymbol{P}_3+\boldsymbol{P}_4)$ and takes the square. It follows

$$\lambda_{21}(1-\varepsilon_4)=\frac{m_1+m_2+m_3}{m_1+m_2}\frac{\varepsilon_3}{h_3} - \frac{\sqrt{m_3 m_4}}{m_1+m_2}\sqrt{\frac{\varepsilon_3\varepsilon_4}{h_3 h_4}}\cos\theta_3+\frac{m_3}{(m_1+m_2)}\frac{\varepsilon_4}{h_4}. \tag{19}$$

We are now able to complete the kinematical diagram also for the cases where *two or three equal particles* are emitted and the detectors do not discriminate between them, but for their energy. This is the case in the specific reactions discussed here: one of the α-particles may be the first one, the other one being emitted, when the remaining group ^{5}He disintegrates into a neutron and the second α-particle. The first α-particle, however, carries a fixed amount of energy in this case, determined by two-particle kinematics. Therefore this case is represented in the ε_1, ε_2-diagram by a vertical straight line. Its position may be read from Eq. (19) when one identifies λ_{12} with the energy contents of ^{5}He and the angle θ_3 with the fixed angle θ_1.

Finally, it is possible that the detector at the fixed position θ_1 detects the α-particle from the decay of ^{5}He, whereas the movable detector no. 2 records the α-particle from the first step of the reaction. The correspond-

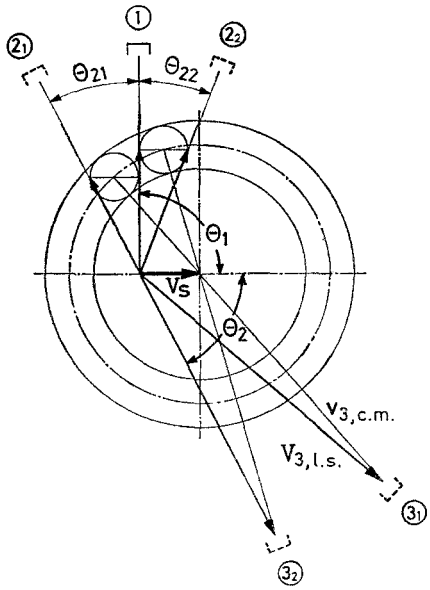

Fig. 6. Angular configurations that are to be considered when two or three particles are identical. *1* fixed detector, *2* and *3* movable detectors. Combination *1* and *2* measures the particles of the subsystem (12), combination 1 and 3 one particle from (12) and the "first" particle 3. The same combination is measured when the first particle is emitted in direction θ_1. θ_{21}, θ_{22}: limiting angles if λ_{12} is rather large

ing curve for constant λ is again a closed curve where λ_{12} is determined by the energy contents of ^{5}He and all the other relations can be used after proper permutations of the pertinent masses. We refer to Fig. 6 where the various combinations of angular positions have been sketched.

4. Discussion and Application to the Reactions ^{7}Li $(d, n)2\alpha$ and ^{7}Li $(d, \alpha)n\alpha$

Eqs. (11) and (16) are the basic results, that may be adapted to any specific problem. Figs. 2, 3 and 5 have already on purpose been drawn for application to the ^{7}Li+d reactions. Since, on the other hand the equations are completely general one may discuss any detail of interest.

Scanning through the known data of levels of ^{8}Be and ^{5}He [1] it becomes clear immediately that there will be no difficulty in separating the ground-state contribution of ^{8}Be or the one of its first excited state (the latter one we have included in the following figures, though).

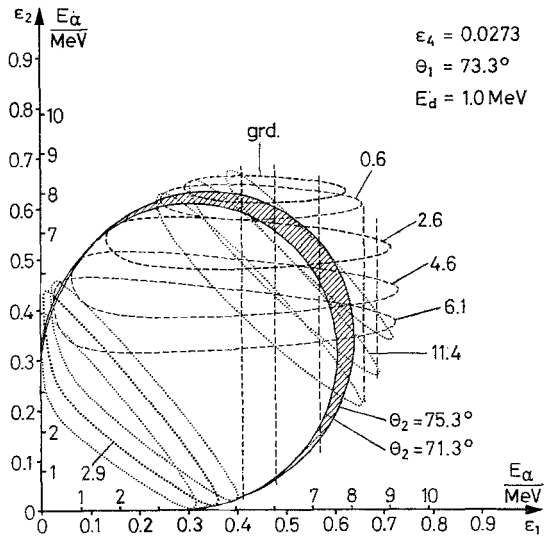

Fig. 7. Kinematical curves and constant—λ-curves for all possible kinematical configurations of the reaction of deuterons with ^{7}Li, leading to α-particles. A tentative first excited state of ^{5}He at 2.6 MeV has been assumed, and an arbitrarily chosen state at 6.1 MeV. Width of the 2.6 MeV state assumed 4 MeV. ^{8}Be-states are indicated by the numbers 11.4 and 2.9. Incoming deuteron energy 1.0 MeV. In the experiment that has been performed, Ref. [6], the angles θ_1 and θ_2 were chosen so that only one λ-branch (the outer one with respect to the center of coordinates) contributed to the counting rate

Fig. 7 contains an energy diagram as it can be obtained from the results of this paper. The experimental conditions of the paper of Hofmann and Kamke [6], were chosen where the fixed detector was set up at 73.3° with respect to the incoming particle beam of 1 MeV energy. In order to properly take account of the finite solid angle of the detectors, the angles 71.3° and 75.3° were taken for drawing the kinematical curves that belong to the experiment. The prediction then is, that all coincident events of interest lie in the hatched area. Constant λ-curves that belong to states of ^{8}Be or ^{5}He are also found in the figure. It now becomes clear that the main difficulty, namely overlapping of coincidence rates, is increased quite substantially, because of the finite velocity of the c.m. It causes the curves of constant λ to spread apart and cover a larger area in the energy diagram compared with the representation in the c.m. system. Only the vertical straight lines maintain favorable conditions, in spite of their moving towards lower energies. When moving along a kinematical curve every point can be labeled with three energies of excitation of subsystems: ^{8}Be*, ^{5}He* and—because of possible inter-

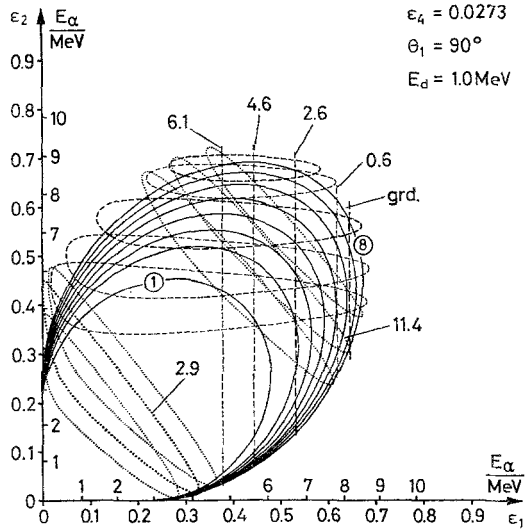

Fig. 8. Energy-diagram pertinent to the experimental situation of Gil *et al.*; incoming particle energy 1.0 MeV. ① ... ⑧ kinematical curves. ①: $\theta_2 = 102.5°$, then beginning with 97.5° in steps of 2.5° to curve ⑧ with $\theta_2 = 82.5°$. In the experiment that has been performed only the inner λ-branch (with respect to the center of coordinates) contributed to the counting rate

change of particles – again ^{5}He*. Any decision on whether the detected counting rate uniquely belongs to one of these system can only be made from the distribution of counts.

The preceding discussion leads to the conclusion that one should take as low a velocity of the center of mass as possible. This procedure is often forbidden by the then decreasing yield of the reaction. In order to give an impression of the expected change of energy diagrams we plot in Figs. 8 and 9 pertinent relations for two different energies of the incoming particle beam. Fig. 9 exactly corresponds to the experimental setup of Gil *et al.* [2], whereas Fig. 8 to the one chosen by Assimakopoulos *et al.* [5]. Since in the latter paper data of the first excited state of ^{5}He are given that are far from data of other groups, their plot of coincidences was compared with Fig. 8. It was found that the location of the first excited state at around 2 ... 2.5 MeV would be compatible with the experimental data.

Finally it should be emphasized that kinematical considerations are only one part of the problem and only give some means to decide on most favorable experimental conditions. They may show that only an

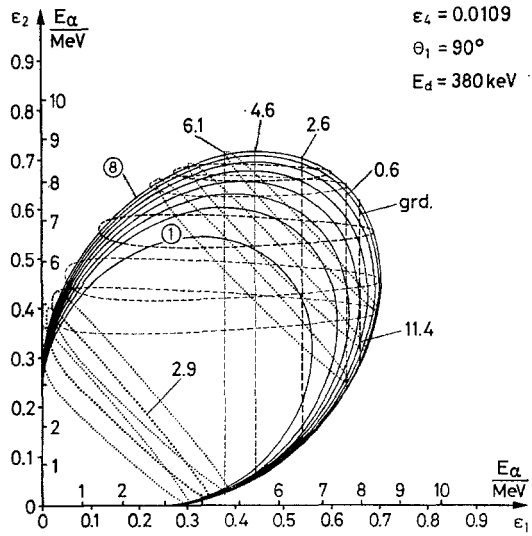

Fig. 9. Energy-diagram pertinent to the experimental situation of Assimakopoulos *et al.*; incoming particle energy 380 keV. Sequence of angles θ_2 same as in Fig. 8

analysis with the simultaneous overlap of three reaction channels allows the determination of spectroscopic data.

Clarifying discussions with J. Krug and S. Haun are gratefully acknowledged. Thanks are also due to Miss B. Hadamik who prepared many plots of various energy diagrams.

Appendix

Calculation of Kinematical Parameters and Energy Variables from Masses and Energies given in the Laboratory System

The reaction is characterized by masses m_a and m_A of the entrance channel, m_1, m_2, m_3 of the exit channel. The reaction energy is defined by

$$Q_3=(m_a+m_A)c^2-(m_1+m_2+m_3)c^2.$$

When the incoming particle energy E_a (laboratory system) is known the total energy T_4 used here is

$$T_4=Q_3+E_a+\frac{m_a}{m_a+m_A}E_a=Q_3+E_a+E_s.$$

In order to calculate the maximum energies one first calculates

$$M_4 = m_1 + m_2 + m_3 + m_s = 2(m_1 + m_2 + m_3).$$

Then for $i=1, 2, 3, 4$ ($s=4$) one defines

$$h_i = \frac{M_4}{M_4 - m_i},$$

thence

$$E_{i,\max} = \frac{T_4}{h_i} = \frac{M_4 - m_i}{M_4} T_4.$$

It follows

$$E_{4,\max} = \tfrac{1}{2} T_4, \qquad \varepsilon_4 = \frac{E_4}{E_{4,\max}} = \frac{2m_a}{m_a + m_A} \frac{E_a}{T_4}.$$

The parameter ε_4 is a fixed number, defined by the incoming particle's energy and the masses.

The inner parameter λ_{12} for the subsystem (12) is defined by

$$e_{12} = (1 - \lambda_{12})(1 - \varepsilon_4)\, T_4.$$

Here e_{12} is the sum of the excitation energy of (12) and the Q-value for the decay of the groundstate, $B_{12} \to b_1 + b_2$. For example $e_{12} = 0.094$ MeV for ^{8}Be (grd.st.)$\to 2\alpha$.

When ε_1 and ε_2 have been found from Eqs. (11) and/or (16) one calculates easily $E_1 = \varepsilon_1 E_{1,\max}$ and $E_2 = \varepsilon_2 E_{2,\max}$, the energies in the laboratory system.

References

1. Ajzenberg-Selove, F., Lauritsen, T.: Nucl. Phys. **78**, 1 (1966)
2. Gil, P., Marquez, L., Québert, J. L., Sztark, H.: Phys. Radium **33**, 315 (1972)
3. Strauss, L., Friedland, E.: Z. Physik **250**, 370 (1972)
4. Fessenden, P., Maxson, D. R.: Phys. Rev. **133**, B71 (1964)
5. Assimakopoulos, P. A., Gangas, N. H., Kossionides, S., Democritus, N. R. C.: Phys. Lett. **19**, 316 (1965); Nucl. Phys. **81**, 305 (1966)
6. Hofmann, G., Kamke, D.: Z. Physik **224**, 446 (1969)
7. Milone, C., Potenza, R.: Nucl. Phys. **84**, 25 (1966)
   Jeremie, H., Martin, Ph., Calamand, A.: Nucl. Phys. A**105**, 689 (1967)
   Juna, J., Konecný, K.: Proc. Conf. Nuclear Reactions, Rossendorf, p. 195, 1966
8. Valković, V., Jackson, W. R., Chen, S. S., Emerson, S. T., Phillips, G. C.: Nucl. Phys. A**96**, 241 (1967)
9. Dehnhard, D., Kamke, D., Kramer, P.: Phys. Lett. **3**, 52 (1962); Ann. Physik **14**, 201 (1964)

10. Kamke, D.: Evaluation of Dalitz Plots, Part I: Inv. Paper, Conf. Clust. Phen. in Nuclei, Bochum 1969. Part II: Ann. Physik (7) **28**, 193 (1972). See also Haun, S., Kamke, D.: Ann. Physik (7) (1973), in print
11. Treado, P. A., Lambert, J. M., Alessi, V. E., Kane, R. J.: Nucl. Phys. A**198**, 21 (1972)

Prof. Dr. D. Kamke
Institut für Experimentalphysik
Ruhr-Universität Bochum
D-4630 Bochum
Universitätsstraße, Gebäude NB
Federal Republic of Germany